Defect Analysis of installed PV-Modules - IR-Thermography and In-String Power Measurement

Claudia Buerhop, Hans Scheuerpflug, Tobias Pickel
Bavarian Center for Applied Energy Research (ZAE Bayern), Haberstraße 2a, D-91058 Erlangen, Germany
email: claudia.buerhop-lutz@zae-bayern.de, Tel.: (+49)9131-9398-177, Fax: (+49)9131-9398-199
Author for correspondence: Claudia Buerhop

Abstract
Inspecting installed PV-modules with IR-thermography is a frequently used method nowadays. Modules with defects, that heat up under operating conditions, can easily be identified. The electric and thermal performance of these defect modules will be studied under operating conditions. Here, the module temperature and its temperature distribution as well as the series connection and the resulting string operating point are of importance. In order to measure the electric current and voltage of every module within a string a special measurement unit linked with an IR-camera was developed. The temperature distribution and the module powers were monitored simultaneously. The data evaluation showed that the module power differs from that measured under STC –conditions. The temperature at the defect site increases with string length and the power decreases respectively. Both, temperature and power approach a certain limiting value.

Keywords: thermography, defect temperature, IR-imaging, module power.

INTRODUCTION

Industrial inspection of PV-plants gains importance. IR-thermography is a valuable tool for quality control [1-6]. There are several advantages. IR-imaging is contact-free, nondestructive, provides two-dimensional images, and can be carried out during operating conditions. Using aerial, drone-mounted camera systems even enhance the inspection [7-9]. Meaningful images require certain measurement conditions, like avoiding shading, partial shading and all types of reflections [10] [11]. Qualitative quality control is enhanced. Irregularities in the IR-images of PV-modules are a strong indication for defective sites, as described elsewhere [12].

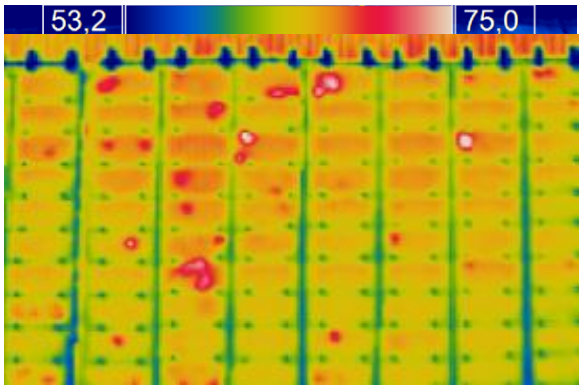

Figure 1: IR-image of a PV-plant section on an industrial roof 67 kW_p showing a large number of modules with elevated temperature, ambient temperature T_{amb} = 35°C, solar irradiance E = 1000 W/m²

The scope of this paper is the enhancement of the interpretation and understanding of IR-images of PV-plants, as seen in Figure 1. The relevance of the series connection for the defect analysis and module performance in terms of power output and temperature development will be pointed out. Therefore simulative studies and field experiments are carried out. Here, the measurement of the IV-curve, of the power output of the module will be of great importance. Table 1 lists different alternatives to measure the module power output.

Table 1: Different power measurements

	Measure-ment conditions	Number of modules	Comment
Sun simulator	STC 1000 W/m², 25°C	Single module	Module and defect at equal and constant temperature
Outdoor IV-curve	T_{amb}, E variable	Single module	Module at operating temperature
Outdoor string measurement unit	T_{amb}, E variable	Up to 20 modules of a string	Modules at operating point, module and defect at operating temperature

EXPERIMENTAL PROCEDURE

Crystalline modules from different manufacturers and different power classes and dimensions were investigated, see Table 2. There were modules with and without defects. All modules were entirely characterized in the lab with regard to defect type and output power (STC). EL-imaging was carried out with high resolving Si-camera CoolSamBa HR-830 with 8.3 MPixel (Sensovation). The format of the detector was 3326 x 2504 pixels. The modules are excited with an external power supply. The applied current was close to the short circuit current. The IV-curves were measured using an AAA sun simulator SIM 4600 SLP (SPIRE).

Table 2: Specification of investigated modules

Module	Nominal power	Number of cells
Type I	80 W	36
Type II	200 W	60

The pre-characterized modules were mounted in an outdoor test facility. The data recording included: weather data; like solar irradiance, ambient temperature, wind velocity, and module data as temperature at certain spots and the operating point. Temperature was measured with an IR-camera Optris PI450 (382 x 288 Pixel). Using the IR-image the temperature distribution across the module could be recorded, too. The operating point, especially the current, was measured at the string inverter. The voltage of the modules while serial connected is measured with a specially developed measuring unit. The modules were kept at maximum power point mpp and the data were recorded.
For analyzing the influence of the string length on the module and string performance with respect to power output and operating current, the number of electrically connected modules is increased stepwise. The string length is n and reaches from 1 (just the defect module) to 20 (1 defect module plus 19 good ones). The set of measurements was done at stable weather to ensure the same ambient conditions.

RESULTS

Simulative Results

For simulating the influence of the serial connection on the module performance LTspice was used. The solar cells were simulated by a simple 1-diode model. The cell defects investigated were soldering faults and cell fracture. A module of type I was supposed to be defect. The simulated IV-curve of a defect and defect-free module is shown in Figure 2. The defect simulated is a bad solder joint.
Table 3 lists the resulting module power and current at mpp.

Table 3: Module data extracted from simulation

	Defect-free module	Defect module
P	80 W	49,9 W
I_{mpp}	4.6 A	3.7 A

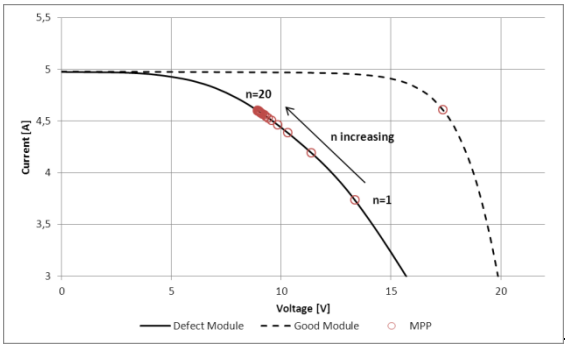

Figure 2: Simulated IV-curve for a good, defect-free module and a defect module (bad solder joints). Mpp is marked for both modules, additionally the shift of mpp with increasing string length n is shown for the defect module.

For studying the influence of the serial connection a module string length up to n = 20 is simulated. The influence on the string power and on the operating string current is analyzed by a stepwise lengthening of the string. As IV-curves in Figure 3 show, the current at the string operating point (at string mpp) increases and approaches I_{mpp} = 4.6 A of the defect-free module.

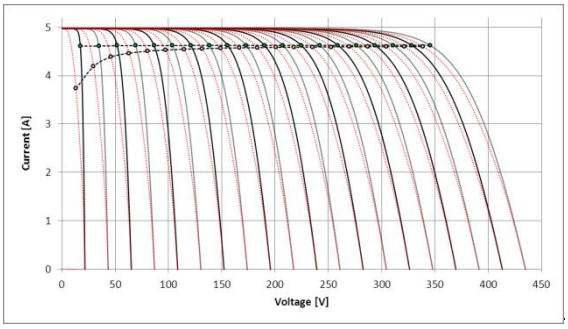

Figure 3: Simulated IV-curves for a defect module (bad solder joints) with increasing number of modules connected in series showing the shift of the current at the resulting string mpp

The generated power of string with length n is given in Figure 4. For n = 3 (1 defect module + 2 good modules) the power loss compared to an ideal string is calculated to be roughly 15% and decreases with increasing string length for n = 10 it is about 5% and for n = 20 almost 2%.

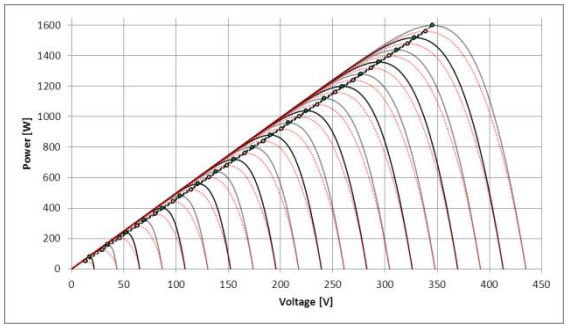

Figure 4: Simulated power curves for a defect module (bad solder joint) with increasing number of modules connected in series showing the shift of the power at the resulting string mpp

The power and current development for the defect module is shown in Figure 5. Since the operating current of the string increases, the current through the defect module increases, too. It approaches the mpp current 4.6 A of a good module. Because of the increase of the operating current, compare Figure 2, the voltage at mpp drops and accordingly the power output is reduced and approaches a fairly constant value for a large number of modules.

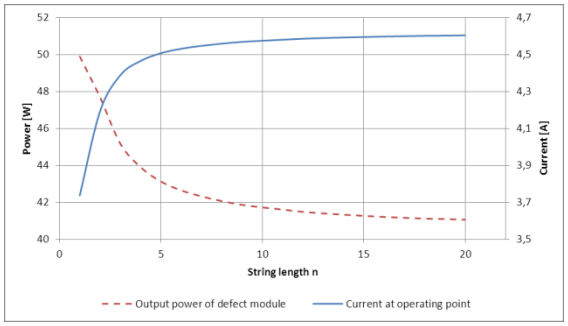

Figure 5: Power and operating current of the defect module (bad solder joint) with increasing number of modules connected in series extracted from the simulated data

Evaluating the simulative data the dissipated power at the defect site and unaffected areas can be estimated. Figure 6 shows that the dissipated power at the defect site increases strongly while unaffected surrounding areas remain at a low level. This increase in dissipated power lead to local temperature rise and so called hot spots.

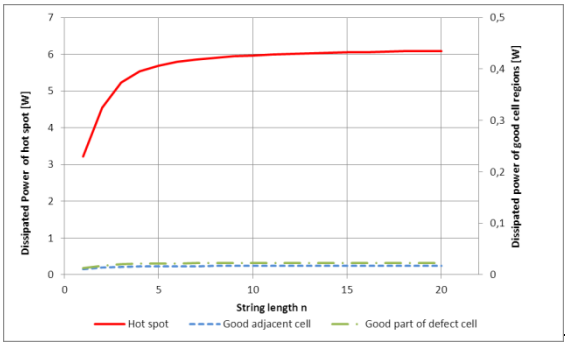

Figure 6: Simulated power losses at the defect site and cell area of the defect cell and the unaffected cell area of a good adjacent cell

Experimental Results

Temperature measurement

Demonstrating the influence of the string length on the temperature distribution, measurements for n =1 to n = 10 were carried out at comparable ambient conditions. The modules were hold at mpp. IR-images for different string lengths are shown in Figure 7 with the same colour scale. While the defects appear fairly light for n = 1, they become outstanding for n = 3 and n= 10, where more modules are serially connected.

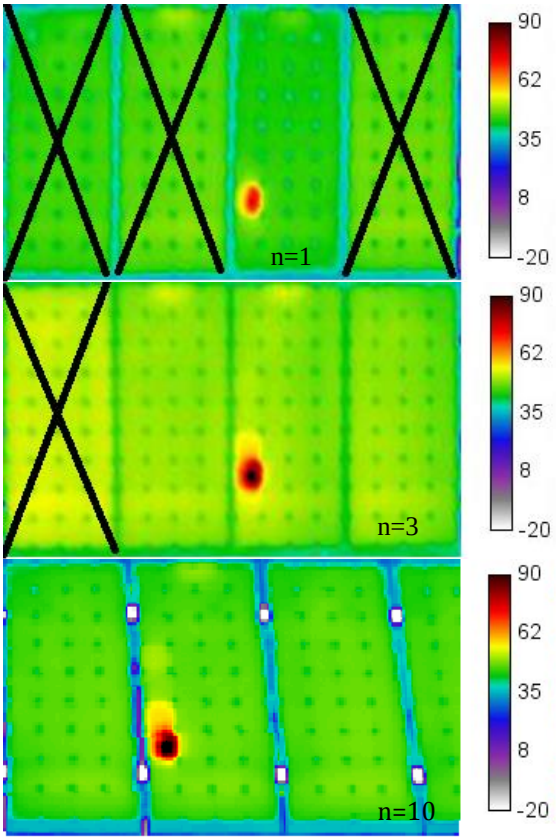

Figure 7: Measured IR-images of a module with one outstanding cell, defect module standing alone (on top), serially connected with two modules (in middle) and serially connected with nine modules

(at the bottom) showing a temperature rise, T_{amb} = 25°C, E = 940 W/m²

The defect temperature increases strongly with increasing n as well as the temperature difference between the defect and the surrounding increases, see Figure 8. The temperature increase can vary and is determined by the defect characteristics.

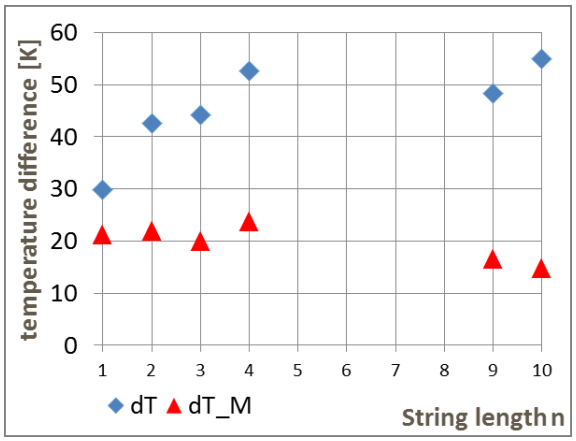

Figure 8: Measured temperature differences at for various string lengths (compare Figure 7), $dT = T_{defect} - T_{ref.cell}$, $dT_M = T_{ref.cell} - T_{amb}$

In agreement with the simulated results, the defect temperature difference increases significantly with small numbers of modules connected in series. For longer string lengths it approaches steadily a constant value. The temperature of adjacent non-defect cells as well as their temperature differences to the ambient temperature are unaffected by the string length.

Power measurement of modules within a string under STC conditions

First, IV-curves of individually measured modules and short strings n < 4 are presented in Figure 9. The behavior for I_{mpp} as expected from the simulative results is visible. I_{mpp} of the string increases towards I_{mpp} of the good module. Therefore more current flows through the defect module and the defect temperature increases (Figure 7, Figure 8). The I_{mpp}-shift involves a significant reduction of V_{mpp}. The consequence is a much lower string output.

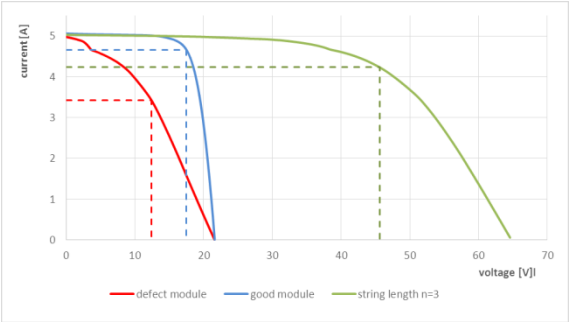

Figure 9: Measured IV-curves of three individually measured modules a good one and a damaged one and a module string n=3 at E = 1000 W/m². The dashed lines indicate I_{mpp} and U_{mpp} of the three measurements. Data correspond to modules from Figure 7.

Power measurement of modules within a string under operating conditions

The influence of the string length on the module performance, e. g. the electrical parameters, is studied using the measurement unit. The measured string data are shown in Figure 10 in comparison with power measurements of the individual module under STC and field conditions. The power for single module depends strongly on the measurement conditions

$$P(STC) > P(field) > P(field, mpp).$$

Reasonable explanations are die differing temperature distribution within the module. At STC all the cells are at 25°C, at the field measurement the cells are at a constant elevated temperature and for the power measurement at maximum power point (mpp) all cell are at their operating temperature (that means the defect cell is heated up).

Connecting the defect module in series with good modules current, voltage and power output changes. As expected, the current through the defect module increases steadily up to the limiting value of I_{mpp} of the good modules. As described above, the module voltage is decreased. As a result, the power output decreases, too.

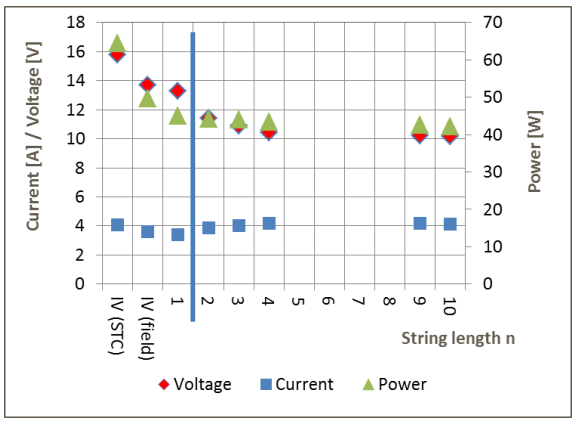

Figure 10: Measured current, voltage, and power output of the defect module for different string lengths under operating conditions $T_{amb} \approx 25°C$, E = 900 – 1000 W/m². Data correspond to modules from Figure 7 and Figure 8

Regarding the string output power, it is observed, that it steadily increases and approaches an output power below that of a string composed only of good modules, see Figure 11.

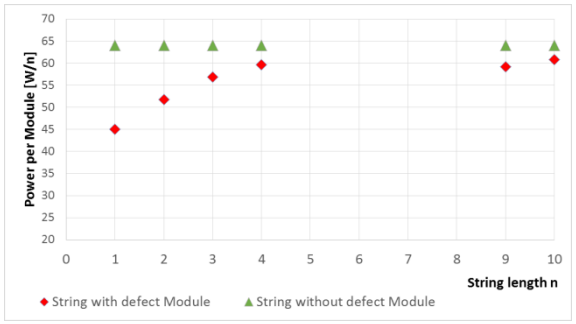

Figure 11: string output power per module as a function of the string length, $T_{amb} \approx 25°C$, E = 900 – 1000 W/m².

DISCUSSION

The measurements and simulations reveal that under real operating conditions the module performance is driven by the existing temperature distribution and the series connection with other modules in a string. Therefore the operating point shifts according to the IV-curves of the connected modules. While the defect temperature usually rises, the power output decreases. The change varies with the defect type and its characteristics. Thus, solder defects may have a minor impact on the string power than cell fracture but nevertheless high local temperatures may result. Here, material damage and fatigue are promoted. Furthermore, the module parameters are of importance. First investigations of high performing modules with larger nominal power show similar performance.

Table 4: power reduction of defect module and module string including one defect module compared to a non-defect module and respectively a string consisting only of good modules, measured and scaled-up data

conditions	Defect module	Module string n=3	Module string n=10
STC n=1	20% Meas.	6.7% Scale-up	2.0% Scale-up
STC n=3	-	8.1% Meas.	-
Amb. Cond. 25°C, n=1, 900-1000°W/m²	29,7% Meas.	9.9% Scale-up	3.0% Scale-up
Amb. Cond. 25°C, n=10, 900-1000°W/m²	34,6% Meas.	11.5% Meas.	4.7% Meas.

The potential influence of defect modules on the string output, here the power reduction with respect to a good module or string, is listed in Table 4. The power for one module is measured under STC conditions with a sun simulator, under ambient conditions with an electronic load or the measurement unit. Using the sun simulator and the measurement unit the measurement of string power up to a certain length was possible. Otherwise a simple scale-up by adding the specific module powers was done. The data reveal that the module output decreases under ambient conditions and in the series connection with other modules drastically. Considering the string length, it is obvious, that the power reduction decreases with increasing string length. However, under operating conditions almost 5% string power reduction results by a module power of 80%.

CONCLUSION

Concluding, IR-imaging is a valuable tool to identify power reducing PV-modules within a string. The module power output under real operating conditions differs from that measured under STC conditions.

ACKNOWLEDGEMENT

We gratefully thank the German Federal Ministry for Economic Affairs and Energy (BMWi) for financial funding this project.

REFERENCES

[1]E. Molenbroek, D. W. Waddington and K. A. Emery, Photovoltaic Specialists Conference, 22nd IEEE (1991) 547.

[2]W. Herrmann, W. Wiesner and W. Vaassen, Photovoltaic Specialists Conference, 1997., Conference Record of the Twenty-Sixth IEEE (1997) 1129.

[3]D. L. King, J. A. Kratochvil, M. A. Quintana and T. J. McMahon, Photovoltaic Specialists

Conference, 2000. Conference Record of the Twenty-Eighth IEEE (2000) 1487.
[4]J. Wohlgemuth and W. Herrmann, Photovoltaic Specialists Conference, 2005. Conference Record of the Thirty-first IEEE (2005) 1062.
[5]R. Auer, U. Jahn, C. Buerhop, C. Vodermayer, G. Wotruba, M. Zehner and M. Niess, 22nd PVSEC (2007) 2519.
[6]U. Jahn, C. Buerhop, U. Hoyer, B. Lerche and S. Wittmann, ep Photovoltaik aktuell (2008) 32.
[7]C. Buerhop and H. Scheuerpflug, 29th PVSEC (2014) 2975.
[8]C. Buerhop and H. Scheuerpflug, Radiometric study of installed PV using aerial thermography (2015) in preparation.
[9]C. Buerhop and H. Scheuerpflug, Third Southern African Solar Energy Conference SASEC (2015) 224.
[10]C. Buerhop, U. Jahn, U. Hoyer, B. Lerche and S. Wittmann, Abschlußbericht der Machbarkeitsstudie zur Überprüfung der Qualität von Photovoltaik-Modulen mittels Infrarot-Aufnahmen (2007) www.zae-bayern.de.
[11]C. Buerhop, H. Scheuerpflug and R. Weißmann, 26th PVSEC (2011) 3413.
[12]C. Buerhop, D. Schlegel, M. Niess, C. Vodermayer, R. Weißmann and C. J. Brabec, Solar Energy Materials and Solar Cells 107 (2012) 154.